

**The Effect of Intensity Windowing on the Detection of Simulated Masses  
Embedded in Dense Portions of Digitized Mammograms in a Laboratory Setting**

Etta D. Pisano, MD\*#  
Jayanthi Chandramouli`  
Bradley M. Hemminger, MS\*  
Deb Glueck, MS^  
R. Eugene Johnston, PhD\*  
Keith Muller, PhD^  
M. Patricia Braeuning, MD\*#  
Derek Puff, PhD`//  
William Garrett, MS@  
Stephen Pizer, PhD\*#@

From the Departments of Radiology\*, Computer Science@, Biomedical Engineering`,  
and Biostatistics^.

The University of North Carolina-Chapel Hill.

School of Medicine, School of Public Health and College of Arts and Sciences.

//Current affiliation, Picker International, St. David's, PA.

Member, UNC-Lineberger Comprehensive Cancer Center #

Supported by NIH PO1-CA 47982, NIH RO1-65583 and DOD DAMD17-94-J-4345

## **Abstract**

### **Purpose:**

To determine whether intensity windowing (IW) improves detection of simulated masses in dense mammograms.

### **Materials and Methods:**

Simulated masses were embedded in dense mammograms digitized at 50 microns/ pixels, 12 bits deep. Images were printed with no windowing applied and with nine window width and level combinations applied. A simulated mass was embedded in a realistic background of dense breast tissue, with the position of the mass (against the background) varied. The key variables involved in each trial included the position of the mass, the contrast levels and the IW setting applied to the image. Combining the 10 image processing conditions, 4 contrast levels and 4 quadrant positions gave 160 combinations. The trials were constructed by pairing 160 combinations of key variables with 160 backgrounds. The entire experiment consisted of 800 trials. Twenty observers were asked to detect the quadrant of the image into which the mass was located.

### **Results:**

There was a statistically significant improvement in detection performance for masses when the window width was set at 1024 with a level of 3328.

### **Conclusion:**

IW should be tested in the clinic to determine whether mass detection performance in real mammograms is improved.

## **Background and Significance**

Effective image display allows for an improvement in the clarity of structural details. Mammography, especially in patients with dense breasts, is a low contrast examination that might benefit from increased contrast between malignant tissue and normal dense tissue. Image processing may allow for improved visualization of details within medical images [1]. Our overall aim is to improve the accuracy of mammography with image processing since as many as 10% of palpable breast cancers are not visible with standard mammographic techniques[2].

Contrast enhancement methods accentuate or emphasize particular objects or structures in an image by manipulating the gray levels in the display. This is done by imposing a predetermined transformation that amplifies the contrast between structures and effectively “resamples” the recorded intensities to enhance the properties of the displayed image [3]. These methods are not designed to increase or supplement the inherent structural information in the image, but simply improve the contrast and theoretically enhance particular characteristics [4]. Intensity Windowing (IW) is an image processing technique that involves the determination of new pixel intensities by a linear transformation which maps a selected band of pixel values onto the available gray level range of the display system [4].

Many investigators have studied the application of digital image processing techniques to mammography. McSweeney tried to enhance the visibility of calcifications by using edge detection for small objects, but never reported any clinical results [5]. Smathers showed that intensity band-filtering could increase the visibility of small objects compared to images without such filtering [6]. Chan used unsharp masking (an edge-sharpening technique used in photography for many years) to remove image noise for computerized detection of calcification clusters [7]. Chan noted that while these techniques improved detection, the improvements may have been greater if the observers had been trained to make diagnoses from the processed mammograms rather than the unprocessed (normal) mammograms [8]. Hale et al. have applied non-specific contrast and brightness adjustment through Adobe Photoshop® to digitized mammograms and have found improved performance by radiologists in determining the likelihood of malignancy of mammographically apparent lesions [9]. Yin et al. showed that nonlinear bilateral subtraction is useful in the computer-detection of mammographic masses [10,11].

Previous work at UNC has explored the use of Intensity Windowing (IW) and the Adaptive Histogram Equalization (AHE) family of algorithms in mammography and computed tomography [12-14]. We have previously described a laboratory-based method for testing the efficacy of an image processing algorithm in improving the detection of masses in dense mammographic backgrounds [15]. With that method, upon which our current work is based, radiologists and non-radiologists exhibit similar trends in detection performance. While non-radiologists did not perform as well as radiologists overall, the two populations displayed parallel increases and decreases in performance due to image processing.

The experiments described in this paper were performed to determine whether IW

could improve the detection of simulated masses in dense mammograms in a laboratory setting. While the scope of this paper is limited to the evaluation of observer performance using our established experimental paradigm, it may be interesting for follow-up work to evaluate these results with respect to measures proposed by other authors, such as the conspicuity measure proposed by Revesz and Kundel. (16-18)

## **Materials and Methods**

The experimental paradigm reported here is based on the model we have previously described and allows for the laboratory testing of a range of parameter values (in this case, window width and level) [15]. The experimental subject is shown a series of test images that consist of an area of a dense mammogram with a simulated mass embedded in the image in one of its four quadrants. The observer's task is to determine in which quadrant the mass is located. The test images are displayed in both the processed and unprocessed format, and the contrast of the object is varied from quite easy to detect to impossible to detect.

A computer program randomly selected one of 40 background images and rotated that background to one of four orientations. The 40 background images of 256x256 pixels each were extracted from actual clinical film screen mammograms digitized using a Lumisys digitizer (Lumisys, Inc. Sunnyvale, CA) with a 50 micron sample size with 12 bits (4096 values) of density data per sample. The images contained relatively dense breast parenchyma. They were known to be normal by virtue of at least three years of normal clinical and mammographic follow-up. They were selected by a breast imaging radiologist from digitized film screen craniocaudal or mediolateral oblique mammograms. Figure 1 shows one of the backgrounds.

These 40 images and four orientations provided 160 different dense backgrounds. Next, the program added a phantom feature (a mass) into the background. The image was processed with IW to yield the final stimulus.

Mammographic masses were simulated by blurring (via convolution with a Gaussian kernel with a standard deviation of 2.0 pixels) a disk that is approximately 5mm in diameter (1.51 degree visual angle at a 38 cm viewing distance). The masses were added at four fixed contrasts. The four contrasts added were, in digitized density units, 20, 40, 80, and 160 digital driving levels (DDLs). While contrast is commonly defined as a change in luminance with respect to the background luminance, we used only the change in luminance in this experiment because the change was independent of the background luminance. This is because contrast was represented in log luminance (i.e. the DDLs corresponded to optical density), and since all the study backgrounds were in the luminance range where Weber's law holds, adding a mass of constant density equates to a constant change in contrast, independent of the background luminance. Although the simulated structures were not entirely realistic, they did, however, possess the same scale and spatial characteristics of actual masses typically found at mammography. Figure 2 shows an example of a simulated mass. Figure 3 shows a typical background image with the mass added to it. We used simulated features instead of real features so that we could have precise control over the location, orientation, and figure to background contrast of the masses.

A three by three (3x3) grid of window and level parameters was designed based

on the results of pilot preference studies done with two radiologists who specialize in breast imaging. In these pilot studies, the two radiologists reviewed dense mammograms with real clinical lesions that were judged to be difficult to visualize using standard film screen mammography. There were 7 images of this type reviewed with 70 combinations of window width and level applied. The radiologists scored each combination of values as showing no change over the standard image, improving the visibility of the lesion, or worsening its visibility.

For experiment 1, the grid spanned all the likely optimal settings (windows of 512, 768, 1024 and levels of 3072, 3328, 3584). Thus, there were a total of 10 IW settings (including the default unprocessed image, with Window width= 4096, Level = 2048) that were applied throughout experiment 1.

To confirm the results of the first experiment and to examine additional IW settings, experiment 2 was performed. Experiment 2 also included the unprocessed (wide open window width) condition and 9 other IW conditions. The combinations of parameters evaluated in Experiment 2 were as follows: window width of 640 with levels of 3456, 3584 and 3840; window width of 1024 with levels of 3200, 3328 and 3584; and window width of 1536 with levels of 2944, 3072, and 3328).

The digital images were printed onto standard 14X17 inch single emulsion film (3M HNC Laser Film, 3m, St. Paul, MN) using a Lumisys Lumicam film printer (Lumisys Inc, Sunnyvale, CA). Each original 50 micron pixel was printed at a spot size of 160 microns, which produced film images 4X4 centimeters, resulting in an enlargement by a factor of three. The radiologist observers in the pilot experiment reported that the magnification did not make the backgrounds unrealistic. Forty images were printed per sheet of film. The images were randomly ordered into an 8X5 grid on each sheet of film. Both the film digitizer and film printer were calibrated, and measurements of the relationship between optical density on film and digital units on the computer were determined in order to generate transfer functions describing the digitizer and film printer. In order to maintain a linear relationship between the optical densities on the original analogue film and the digitally printed film, we calculated a standardization function that provided a linear matching between the digital and printer transfer functions. This standardization function was applied when printing the films to maintain consistency between the original optical densities of the original mammography film and those reproduced on the digitally printed films. The film printer produces films with a constant relationship between an optical density range of 3.35 OD to 0.13 OD, corresponding to a digital input range of 0 to 4095, respectively.

There were 20 observers for each experiment. These were graduate students from the medical school, biomedical engineering department, and computer science department. Performance bonus pay was provided. Observers selected the quadrant of the image that they thought contained the mass. All images contained a mass. Observers were told to make their best guess if they could not see the simulated mass with certainty.

Films were displayed in a darkened room on a standard mammography lightbox that was masked so that only the grid of images on the film was illuminated. Observers could move closer to the image and could use a standard mammography magnifying glass, as desired. The observers were trained for the task through the use of two sets of stimulus image films with instructive feedback before actually starting the experiment.

Both experiments had the same basic design. The order of the presentation of the stimuli was counterbalanced so as to eliminate any systematic effect of non-important variables. All 160 possible combinations of processing condition (10 IW levels), contrast level (4 contrasts) and location of the masses (4 quadrants) were used in the experiment. The experiment was designed to have 5 self-contained blocks, in which all 160 combinations appeared. The intent was to have the observer see all the combinations in each block, in case the observer was unable to complete the experiment. In fact, all observers did complete the experiment. There were 40 backgrounds and 4 possible rotations of each background, for 160 possible background patterns. For each block, a different background pattern was assigned uniquely to each of the 160 possible combinations. The assignment was different for each block. Each observer looked at a total of 800 images, which were the 160 possible combinations, each superimposed on 5 backgrounds.

Observers were instructed to take breaks after each block of stimuli, and more often if necessary. No time limit was imposed on the observers viewing duration of the test images. Overall, the experiment took 2 hours for each observer, divided into two sessions of approximately 60 minutes each. The two sessions were always scheduled on two different days within a week of each other.

### *Data Analysis Overview*

Classical sensory discrimination theory predicts that since contrast values were varied from virtually imperceptible to highly apparent, a typical S-shaped curve will describe the data[2]. At values where the contrast was very low, observers will on average guess randomly and get approximately 25% right since there are four choices. Where the contrast is very high, they will almost always get the correct answer. This relationship between  $\log_{10}$  of the contrast of the object relative to the background intensity and the percent correct can be described with a probit model. This model is typically used to describe the relationship between a continuous predictor (log contrast) and a discrete variable (percent correct), and assumes that the curve between them is described by the cumulative Gaussian distribution.

Probit models were fit for each subject and enhancement condition using contrast (DDLs of mass above background) as the predictor. The probability that a subject gets

$$\Pr\{\text{correct}\} = 1/4 + (1 - 1/4) \Phi [(x - \mu_{ij})/\sigma_i].$$

a correct answer is given by the following equation:

Here  $i$  indexes subjects, and  $j$  indexes enhancements with  $x$  representing the density. For each subject, this gave a separate location parameter estimate for each enhancement, and a common spread parameter estimate. Our assumption is that there is a common spread parameter makes sense biologically, since it corresponds to linearity of the perceptual mapping. It is advantageous to an organism to have the same amount of change in stimulus produce a constant perceptual response, and that

is precisely how the human visual system works over a wide range.

The location parameter,  $\mu$ , is the mean of the corresponding Gaussian distribution and the inflection point of the sigmoidal probit curve. Processing conditions that improve detection will cause this parameter to be smaller, and the curve will shift to the left. This occurs because lower contrast levels are required to spot the object. When the processing of the image makes detection harder, higher contrast levels are needed to locate the mass, and the curve shifts to the right. The values of  $\sigma$ , the spread parameter, correspond to the slope of the line. Large values of  $\sigma$  correspond to steep slopes.

The probit analysis summarized the relationship between contrast and proportion correct for each subject and processing condition. To compare the processing conditions and to examine the effect of window width and level, further analysis was needed. To include both the mean and the location parameter from the probit analysis, we defined an overall measure to be  $\theta_{ij} = \mu_{ij} + \sigma_i$ , which corresponds to 88% correct. Because we were interested in the improvement offered by IW, we measured the "success" of a processing condition by calculating the difference between its  $\theta$  score and the  $\theta$  score for the unprocessed image for each subject. A large positive difference-of- $\theta$  score reflects improved performance, because it indicates better detection with processed images than with unprocessed images.

For each experiment, two analyses were performed using this outcome measure. To keep an overall experiment-wide type 1 error rate of .05, a repeated measures Analysis of Variance was done at the .04 level, with a set of nine T-tests at the .01/9 level.

Repeated measures analysis of variance (ANOVA) is a technique used to analyze data in which many measurements were made on each subject. It allows one to examine the effect of processing conditions and their interactions, while allowing for the dependence of measurements taken on the same observers. With the difference in  $\theta$  scores as the outcome, and window width and level as the predictors, the repeated measures ANOVA model was fitted.

The model can be thought of as a response surface in three dimensions with performance plotted against window width and level. A flat surface would mean that window width and level had no effect on the outcome. The major hypothesis tested in the ANOVA is equivalent to asking the question "Is the response surface flat?". If it is not flat, the step-down hypotheses allow one to ask what shape the surface is, whether it is curved in both directions (quadratic by quadratic trends), curved in one direction and sloped in the other (quadratic by linear trends), or sloped in both directions (linear by linear trends). A peak in the surface means that there is one image processing technique that is better than any other. Conversely, if the difference score is equal to zero for any intensity windowing setting, it would correspond to no difference between the processed image and the unprocessed image. That is what the T statistics test.

## **Results: Experiment 1**

The repeated measures ANOVA revealed that there was a significant interaction between window width and level ( $p=.0001$ ,  $G-G\Lambda = .8347$ ). To examine the nature of this interaction, a series of step-down tests was planned. There was a significant interaction between a quadratic trend in window width and a quadratic trend in level ( $F=31.08$ ,  $p=.0001$ ). Because the quadratic by quadratic interaction was significant, no further tests were examined. A quadratic by quadratic trend means that the surface was curved with respect to both window width and level, and that the shape of the curve differed for fixed levels of window width and level. (Figures 4 and 5).

At the overall .01 level, the differences between the enhancement conditions and the unenhanced were examined. The null hypothesis is that there will be no difference between the mean  $\theta$  for the unenhanced and an enhancement condition. There are nine such hypotheses, corresponding to the nine enhancements. A Bonferroni correction to control the overall error rate made each individual alpha level .0011. Four settings of intensity windowing made finding the masses significantly harder, three made the task significantly easier and two made no significant difference. The settings that made the task easier are window width 1024 with level 3328, window width 768 with level 3584 and window width 1024 with level of 3584. (Table 1)

## **Results: Experiment 2**

Again, the repeated measures ANOVA showed that there was significant interaction between window width and level ( $p<0.0001$ ,  $F=60.9$ ). (Figures 6 and 7) As in experiment 1, a quadratic by quadratic interaction was significant ( $p<0.0001$ ,  $F=32.61$ ). Table 2 shows the results of nine two-sided t-tests. Only one image processing setting resulted in significantly better performance than the unprocessed, namely window width of 1024 with a window level of 3328 ( $p<0.0001$ ). Seven of the settings were not significantly different from the unprocessed image. One setting was significantly worse. (Table 2)

The probit model predicts that IW will increase detection of masses by as much as 17% in cases near the threshold of detection. (Figures 5 and 7).

## **Discussion**

These results are encouraging. This is the first experiment in mammography that demonstrates that an algorithm can improve the detection of a simulated mass placed in a dense mammogram. At the same time, it is obviously important to choose the window width and level with care since performance can be significantly degraded if inappropriate parameters are chosen.

What do these results mean for clinical mammographers? Will we be using this technology in the clinic in detecting lesions in dense mammograms? The use of



graduate student observers and the use of simulated masses in this study might incorrectly predict the performance of radiologists in detecting real masses in real patients. We have demonstrated previously that graduate student performance at this task parallels the performance of experienced mammographers [15]. Evaluation by radiologists on real patients will determine the ultimate utility of this algorithm in the clinical setting. Because we have used real clinical images and we have simulated masses using relatively realistic stimuli, we are optimistic that these methods will improve clinical performance and that radiologists will be using IW to help them in determining whether mammograms of women with dense breasts really do contain masses.

Digital mammography will be available in the clinic very soon. It is obvious that image processing will be used to optimize the visibility of lesions in digital mammograms [20]. Ideally, any image processing algorithm that might be useful will be tested on real patients in that setting. That will be an expensive and time consuming process that will involve real patients making clinically important decisions about their own breast health, including the advisability of biopsy, lumpectomy and mastectomy. Ideally, before this technology arrives in the clinic, radiologists will have some idea of which category of algorithms to test in that setting. This work is intended to give radiologists preliminary data to narrow the choices that might be useful before the expensive clinical tests are undertaken. This approach suggests not only which algorithms might help clinically but which parameter settings most improve detection.

One could take the approach that the IW dials should be spun until a clinically pleasing image is displayed. This approach might be acceptable and even convincing to many radiologists. It is at least possible that what pleases radiologists in terms of the aesthetics of the image might not improve the detection performance of their visual systems, and in fact, could worsen their detection performance. This project was intended to be more rigorous in exploring the window widths and levels that might be useful in the most challenging areas of the breast, namely the dense parts. We have performed similar experiments on the AHE class of algorithms also [21,22].

This experiment does not address how IW would effect the appearance of fatty areas of the breast, and the detectability of lesions in those parts. We would not want to apply an algorithm that degrades performance in areas of the breast where sensitivity is quite high with current technology. There are two possible technical responses to that concern. First, IW could be applied selectively to only the dense areas as an adjunct to the more standard appearing mammogram with the radiologist pointing and clicking to the areas where windowing would be desirable. Alternatively, the IW could be individualized to the patient's unique intensity histogram so that the areas to be processed of the image could be selected by the computer itself. In fact, ideally the computer could be programmed to choose an individual IW setting for each portion of the mammogram so that contrast was preserved in all portions of the image. Ongoing experiments in our laboratory are currently exploring the latter possibility.

Of course, our results to date cannot estimate the exact frequency of false positive

diagnoses when intensity windowing is used. Many alternate forced choice tests (in our case, 4-AFC) yield proportion correct as the primary outcome. MacMillan and Creelman discussed methods for converting proportion correct in this setting to a value of  $d'$ , the sensitivity parameter of an ROC analysis [23]. The particular choice of conversion depends on side conditions concerning the nature of any rater bias. Given the characteristics of the study design, subjects and training, we believe that superior proportion correct will translate into superior  $d'$ . If this is true, the practical value of intensity windowing must be tested in a clinical setting. Then ROC analysis will allow separate analysis of a reader's sensitivity and pay off function on the performance of the technique as part of a diagnostic system.

The testing of these methods on patients with palpable and mammographically detected lesions has been funded by the National Cancer Institute and the Department of Defense, and will be ongoing over the next few years at UNC and Thomas Jefferson University Hospital. We expect to evaluate both Intensity Windowing and Contrast Limited Adaptive Histogram Equalization (CLAHE) in the clinical setting to determine whether or not these algorithms improve the performance of radiologists in detecting and characterizing breast lesions.

## References

1. Rosenman J, Roe CA, Cromartie R, et al. Portal film enhancement: Technique and clinical utility. *Int J Radiat Oncol Biol Physics* **1993**;25(2):333-338.
2. Homer MJ. *Mammographic interpretation: a practical approach*. New York, NY: McGraw Hill, **1991**;4-5.
3. Pizer SM. Psychovisual issues in the display of medical images. K.H.Hoehne, ed., *Pictorial Information Systems In Medicine*. Berlin: Springer-Verlag, **1985**;211-234,.
4. Jain AK. *Fundamentals of Digital Image Processing*. Englewood Cliff, NJ: Prentice Hall, **1989**.
5. McSweeney MB, Sprawls P, Egan RL. Enhanced image mammography. *AJR* **1983**;140:9-14.
6. Smathers RL, Bush E, Drace J, et al. Mammographic microcalcifications: Detection with xerography, screen-film, and digitized film display. *Radiology* **1986**;159:673-677.
7. Chan HP, Doi K, Galhorta S, et al. Image feature analysis and computer-aided diagnosis in digital radiography: I. automated detection of microcalcifications in mammography. *Med. Phys.* 1987; 14(4):538-547.
8. Chan HP, Vyborny CJ, MacMahon H, et al. Digital mammography ROC studies of the effects of pixel size and unsharp-mask filtering on the detection of subtle microcalcifications. *Investigative Radiology* 1987; 22:581-589.
9. Hale DA, Cook JF, Baniqued Z, et al. Selective Digital Enhancement of Conventional Film Mammography. *J Surg Onc* **1994**;55:42-46.
10. Yin F, Giger ML, Vyborny CJ, et al. Comparison of Bilateral-Subtraction and Single-Image Processing Techniques in the Computerized Detection of Mammographic Masses. *Inv Rad* **1993**;28(6):473-481.
11. Yin F, Giger M, Doi K, et al. Computerized detection of masses in digital mammograms: Analysis of Bilateral Subtraction Images. *Med Phys* **1991**;18(5):955-963.
12. Hemminger BM, Johnston RE, Muller KE, et al. Comparison of clinical findings between intensity-windowed versus CLAHE presentation of chest CT images. *SPIE Medical Imaging VI: Image Capture, Format and Display* **1992**;1653:164-175.
13. Pizer SM, Zimmerman JB, Staab EV. Adaptive grey level assignment in CT scan

display. *Journal of Computer Assisted Tomography* **1984**;8(2):300-305.

14. Puff DT, Cromartie R, Pisano ED. Evaluation and optimization of contrast enhancement methods for medical images. *Proceedings of the SPIE Visualization in Biomedical Computing Conference* **1992**;1808:336-346.
15. Puff DT, Pisano ED, Muller KE, et al. A method for determination of optimal image enhancement for the detection of mammographic abnormalities. *J Dig Imaging* **1994**; 7:161-171.
16. Revesz G, Kundel HL, Graber MD. The influence of structured noise on the detection of radiologic abnormalities. *Investigative Radiology* **1974**; 9:479-486.
17. Kundel HL, Revesz G. Lesion conspicuity, structured noise and reader error. *AJR* **1976**; 126:1233-1238.
18. Revesz G, Kundel HL. Psychophysical studies of detection errors in chest radiology. *Radiology* **1977**; 128:559-562.
19. Hemminger, BM, Johnston RE, Rolland JR, Muller KE. Introduction to perceptual linearization for video display systems for medical image presentation. *J Dig Imaging* **1995**;8(1):21-34.
20. Shtern F. Digital mammography and related technologies: a perspective from the National Cancer Institute. *Radiology* **1992**;183(3):629-30.
21. Pisano ED, Hemminger BM, Garrett W, Johnston RE, Chandramouli J, Glueck D, Muller K, Braeuning MP, Puff D, Pizer S. Does CLAHE image processing improve the detection of simulated masses in dense breasts in a laboratory setting? *Association of University Radiologists Meeting*. Birmingham, Alabama, April 19, **1996**.
22. Pisano ED, Hemminger BM, Garrett W, Johnston RE, Zong S, Glueck D, Muller K, Braeuning MP, Puff D, Pizer S. Does CLAHE image processing improve the detection of simulated spiculations in dense breasts in a laboratory setting? *Association of University Radiologists Meeting*. Birmingham, Alabama, April 19, **1996**.
23. MacMillan NA, Creelman CD. *Detection theory: a user guide*. Cambridge, England:Cambridge University Press, **1991**:135-136.

## CAPTIONS:

Figure 1: An example of a dense normal background taken from a patient's mammogram and used in the reported experiments.

Figure 2: An example of a simulated mass. The actual size of the masses used in the experiments was only 5 mm.

Figures 3 a & b: A dense background with a simulated mass embedded in it in the right upper quadrant (arrow). Figure 3a is the default unprocessed image with window width 4096 and level 2048. Figure 3b is the same image with window width 1024 and level 3328.

Figure 4: Interpolated predicted values from repeated measures ANOVA for Study 1: difference in  $\theta$  value versus window width and window level.


Figure 5: Estimated detection probability from Study 1 for window width of 1024 and window level of 3328 versus unprocessed condition. The shift in the curve to the left reflects improved detection.

Figure 6: Interpolated predicted values from repeated measures ANOVA for Study 2: difference in  $\theta$  value versus window width and window level.


Figure 7: Estimated detection probability from Study 2 for window width of 1024 and window level of 3328 versus unprocessed condition. The shift in the curve to the left reflects improved detection.

Table 1: Summary of differences between unenhanced and enhanced theta for Study 1.

Table 2: Summary of differences between unenhanced and enhanced theta for Study 2.

**Table 1: Summary of differences between unenhanced and enhanced  for Study 1.** Positive values in mean difference in  $\theta$  column correspond to improved detection of simulated masses.

Window Level	Window Width	Mean Diff in $\theta$	Std Dev	p-value
3072	512	-.50	.108	.0001
3072	768	-.32	.093	.0001
3072	1024	-.34	.089	.0001
3328	512	-.11	.074	.0001
3328	768	.04	.087	.0706
3328	1024	.18	.104	.0001
3584	512	-.03	.097	.1716
3584	768	.14	.082	.0001
3584	1024	.12	.121	.0004

**Table 2: Summary of differences between unenhanced and enhanced  for Study 2.** Positive values in mean difference in  $\theta$  column correspond to improved detection of simulated masses.

Window Level	Window Width	Mean Diff. In $\theta$	Std Dev	p-value
3456	640	0.04	0.08	0.0239
3584	640	-0.05	0.09	0.0215
3840	640	-0.31	0.09	0.0001
3200	1024	0.04	0.07	0.0142
3328	1024	0.14	0.08	0.0001
3584	1024	0.01	0.09	0.6155
2944	1536	-0.02	0.07	0.1255
3072	1536	0.06	0.08	0.0045
3328	1536	0.06	0.07	0.0013

